International Journal of Engineering Research and Development
e- ISSN: 2278-067X, p-ISSN: 2278-800X, www.ijerd.com
Volume 21, Issue 6 (June 2025), PP 11-24

Hemorheology of Blood flow infused with Alumina and Ferric oxide nanoparticles through an inclined permeable tapered and overlying stenosed Artery

Disu, A. B.[1], Babatunde, A. J.[2*], Dada, M. S.[2], Alamu-Awoniran F. H.[3], Mohammed M. T.[4] and Danas J. Y.[2]

[1]*Department of Mathematics, National Open University of Nigeria, Abuja, Nigeria*
[2]*Department of Mathematics, University of Ilorin, Ilorin, Nigeria*
[3]*Basic Science Department, Babcock University Ilishan Remo, Ogun State, Nigeria*
[4]*School of Early Childhood Care and Primary Education, Federal College of Education (T) Potiskum, Yobe State*
Corresponding author's Email: babatundeabiodunjoseph@gmail.com.

ABSTRACT *This study scrutinizes the impacts of Alumina and Ferric oxide nanoparticles infused in blood flow through an inclined permeable tapered and overlaying stenosed artery. The study utilized Newtonian model of the blood flow, which were the formulated governing equations and first non-dimensionlised to aid analytically solutions and graphically representations of temperature, velocity, flow resistance and the wall shear stress of the blood. These solutions revealed the influence of important parameters vitals in the biomedical field. The outcomes of this study underline the importance of understanding blood flow dynamics in stenosed arteries and the possible benefits of usage of alumina and ferric oxide nanoparticles in treatment schemes. These nanoparticles were designed to target directly specific tissues or cells of the stenosed artery, consequently improving treatment effectiveness and reducing side effects. The interpretations of velocity and temperature profiles provide understanding of the dynamics of the blood flow under different conditions, therefore informing the development of targeted tissues or cells of the artery. Hence, the velocity profiles improved as Darcy number, Grashof number and heat absorption raised, whereas dropped with development of slip parameter and volume fraction of nanoparticles. The temperature profiles increased in the favor of heat absorption. More so, the resistance to flow increased with rising in heat absorption, Grashof number, and slip parameter. The wall shear stress decelerated as Darcy number, slip parameter, heat absorption, and volume fraction of nanoparticles increased. Ferric oxide reacted to the flow than Alumina in velocity and temperature profiles but converse was the case at wall shear stress. All these parameters had significant effects on the blood flow dynamics.*

Keywords*: Alumina and Ferric oxide nanoparticles, Tapered and overlying stenosed artery, Resistance to flow, Wall shear stress*

Date of Submission: 05-06-2025 Date of Acceptance:16-06-2025

I. INTRODUCTION

The word nanoparticles mean very small particles that cannot be seen except with the aid of electronics microscope which ranges from 1-100 nanometres in size. The nanoparticles are used in molecular engineering, nanomaterials, nanosensors, molecular machines, diagnostics and analysis of blood behaviour through Magnetic Resonance Imaging (MRI) techniques and targeted drug delivery. Therefore, nanoparticles are infused in blood stream to study the dynamics of the blood flow, because of their interactions with blood components and vascular walls which can impact the flow pattern and provide more insight into cardiovascular diseases such as atherosclerosis, inflammation or congenital defects.

Consequently, Ahmed and Nadeem, (2016) utilized copper, titanium dioxide and alumina nanoparticles as antimicrobials in blood flow through diseased arteries. The study provided an understanding that addition of nanoparticles improves the dynamics of blood flow in disease vessels and it established antimicrobial characteristics that can aid to avert infections in diseased vessels. Sarwar et al. (2022) established that gold nanoparticles enhanced the thermal conductivity of the blood using sisko non-Newtonian fluid model. The study

developed new medical treatments, such as targeted drug delivery to specific area of the body, including regions with blood flow restriction, potentially improving treatment and thermal therapy.

Ellahi et al. (2014) conducted an examination into non-Newtonian fluid flow to elucidate a composite stenosis through a porous artery. They depicted the flow resistance rises via the influence of stenosis height, however reduces by addition of values of slip parameter and length. They also noticed that partially permeability can be formed known as endothelium, in the inner cellular layers of blood significantly influence the porosity of the artery. The wall shear stress is of prominent important on the blood flow through the arteries and crucial tools in the restoring of the arterial wall Mofrad et al. (2005). Srivastav (2014) elucidated the concept of Newtonian modeled of blood flow through permeable wall stenotic artery and exposed that the resistances flow speedup as the result of raising of the stenosis height, however, the wall shear stress dropped.

Babatunde and Dada (2021a) revealed that the resistance to blood flow reduced with an augmented value in hematocrit level.Babatunde et al. (2021b) juxtaposed the effects of hematocrit on a tapered-overlapping artery. They discovered that the velocity and temperature of the blood flow increased as the value of hematocrit increases. Babatunde and Dada (2024) delved deeply into Casson modeled blood fluid through a tapered-overlapping stenosed artery. They observed that stenosis knows as the narrowing of the internal, external of an artery, mostly lead to atherosclerotic plaque formation, and poses a major risk to cardiovascular health, usually resulted to blood flow constrained and augmented menace of complications such as ischemic strokes, transient or heart attack.

In biomedical investigations, a good number of scholars have explored nanoparticles on stenotic arteries (Jamil et al. 2018 and Vasu et al. 2020). Different authors exploited nanoparticles for their researches, because of tiny size, high surface area and ability to interact at the cellular and molecular level. Some of researchers like Shahzad et al. 2022, Karmakar et al. 2023 and Muthtamilselvan et al. 2023 utilized gold nanoparticles leveraged on their sole visual belongings for exact picture and stalking inside the complicated vascular system. Sharma et al. 2023 opted for Alumina nanoparticles as results of the high surface area, chemical stability, biocompatibility and mechanical strength. They examined the characteristics of the alumina nanoparticles exhibitions within the curved artery and suggested that the nanoparticles could facilitate drug delivery to the targeted cells or tissues. Copper-Alumina nanocomposites are in the study of stenosed artery for synergistic antimicrobial, enhanced biocompatibility, therapeutic coatings and catalysis in drug delivery (Haris et al. 2024). Imperatively, Copper and Alumina nanoparticles are explored for cancer therapy, antimicrobial coating, wound healing, bone generation, biosensing and drug delivery in nanomedicine.

Alumina and Ferric oxide nanoparticles, to be precise, appear as focal mechanisms in this study have their relations with components of the blood and arterial walls. For instance, Ferric oxide nanoparticles can be functionalized with ligands that target atherosclerotic plagues. Also, Alumina nanoparticles may be functionalized with targeting ligands (antibodies, peptides) that bind specifically to receptors expressed in stenosed or inflamed arterial tissues. Inspired by the interactions and functions of Alumina and Ferric oxide in the blood stream, cells and tissues, the present work infused water based fluid, Alumina and Ferric oxide nanoparticles in the study of a tapered-overlying permeable stenosed artery. Exploring the interactions of the nanoparticles, slip parameter, Darcy number, inclination angle, Grashof number, heat absorption constant and tapered stenosed artery.

II. Formulation of the problem

The study considers a steady Newtonian blood flow modeled in fused with Alumina and Ferric oxide through axisymmetric artery. At any point in the blood flow is represented by the cylindrical polar coordinate (r, θ, z), where z is coordinate along the axis of the artery, while r and θ are coordinates along the radial and circumferential directions, respectively.

The mathematical expression for the blood flow corresponding to the geometry of this study is given by Mekheimer et al. 2012.

$$\frac{R(z)}{R_0} = \begin{cases} \left(\frac{mz}{R_0}+1\right) - \frac{\delta cos\,\emptyset}{R_0 L_0}(z-d)\left\{11 - \frac{94}{3L_0}(z-d) + \frac{32}{L_0^2}(z-d)^2 - \frac{32}{3L_0^3}(z-d)^3\right\}, d \le z \le d + \frac{3L_0}{2} \\ \left(\frac{mz}{R_0}+1\right), \qquad otherwise, \end{cases} \quad (1)$$

where $R(z)$ signifies the radius of the tapered arterial segment in the constricted region, R_0 denoted the constant radius of the normal artery in the non-stenotic region, φ represents the angle of tapering, $\frac{3L_0}{2}$ is the length of overlapping stenosis, d denotes the location of the stenosis, $\delta cos\varphi$ is considered as the critical height of the overlapping stenosis and $m = tan\varphi$ symbolizes the slope of the tapered vessel. In order to elucidate the likelihood of the diff erent outlines of the artery, branded as converging tapering ($\varphi < 0$), non-tapered artery ($\varphi = 0$) and the diverging tapering ($\varphi > 0$).

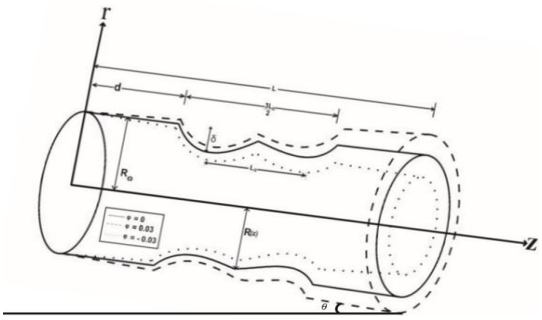

Figure1. The diagram of overlapping stenosed artery.

For a fully developed blood flow in a stoned artery, the equations of the flow and energy equation are given as:

$$\frac{\partial \bar{V}}{\partial \bar{R}} + \frac{\bar{V}}{\bar{R}} + \frac{\partial \bar{W}}{\partial \bar{Z}} = 0 \quad (2)$$

$$\rho_{nf}\left(\bar{V}\frac{\partial \bar{V}}{\partial \bar{r}} + \bar{W}\frac{\partial \bar{V}}{\partial \bar{Z}}\right) = -\frac{\partial \bar{p}}{\partial \bar{R}} + \mu_{nf}\frac{\partial}{\partial \bar{R}}\left(2\frac{\partial \bar{V}}{\partial \bar{R}}\right) + \mu_{nf}\frac{\partial}{\partial \bar{Z}}\left(2\frac{\partial \bar{V}}{\partial \bar{Z}} + \frac{\partial \bar{W}}{\partial \bar{R}}\right) - \rho_{nf}\, g\cos\theta, \quad (3)$$

$$\rho_{nf}\left(\bar{V}\frac{\partial \bar{W}}{\partial \bar{R}} + \bar{W}\frac{\partial \bar{W}}{\partial \bar{Z}}\right) = -\frac{\partial \bar{p}}{\partial \bar{R}} + \mu_{nf}\frac{\partial}{\partial \bar{Z}}\left(2\frac{\partial \bar{W}}{\partial \bar{Z}}\right) + \mu_{nf}\frac{1}{\bar{R}}\frac{\partial}{\partial \bar{R}}\left[\bar{R}\left(\frac{\partial \bar{V}}{\partial \bar{Z}} + \frac{\partial \bar{W}}{\partial \bar{R}}\right)\right] - \rho_{nf}\, g\varrho(\bar{T} - \bar{T}_0) + \sin\theta \quad (4)$$

$$\rho C_p\left(\bar{V}\frac{\partial \bar{T}}{\partial \bar{R}} + \bar{W}\frac{\partial \bar{T}}{\partial \bar{Z}}\right) = k_{nf}\left(\frac{\partial^2 \bar{T}}{\partial \bar{Z}^2} + \frac{\partial^2 \bar{T}}{\partial \bar{R}^2} + \frac{1}{\bar{R}}\frac{\partial \bar{T}}{\partial \bar{R}}\right) + \frac{Q_o}{(\rho c_p)_{nf}} \quad (5)$$

The boundary conditions are as follows:

$$\frac{\partial \bar{W}}{\partial \bar{R}} = 0,\ \frac{\partial \bar{T}}{\partial \bar{R}} = 0 \quad at \quad \bar{R} = 0, \quad (6)$$

$$\bar{W} = v_c,\ \bar{T} = 0 \ at \quad \bar{R} = R(z), \quad (7)$$

$$\frac{\partial \bar{W}}{\partial \bar{R}} = \frac{\alpha}{\sqrt{D_a}}\left(v_s - v_p\right) \quad at \quad \bar{R} = R(z), \quad (8)$$

where $\bar{T}$ represents heat of the fluid,Q_o signifies the heat-absorbing or heat generating element, $v_p = -\frac{D_a}{\mu}\frac{dp}{dz}$symbolizes the velocity in the porous boundary and v_s denotes the slip velocity α and D_a are the Darcy number and the slip parameter respectively.

The thermal attributes of nanofluids by Haris et al. 2024 presented as

$$\left.\begin{array}{c} \frac{\rho_{nf}}{\rho_f} = \left((1-\emptyset) + \emptyset\frac{\rho_s}{\rho_f}\right), \\ \frac{\mu_{nf}}{\mu_f} = \frac{1}{(1-\emptyset)^{5/2}}, \alpha_{nf} = \frac{k_{nf}}{(\rho C_p)_{nf}} \\ \frac{(\rho C_p)_{nf}}{(\rho C_p)_f} = \left((1-\emptyset) + \emptyset\frac{(\rho C_p)_{nf}}{(\rho C_p)_f}\right), \\ \frac{k_{nf}}{k_f} = \frac{k_s + 2k_{bf} - 2\emptyset(k_{bf} - k_s)}{k_s + 2k_{bf} + 2\emptyset(k_{bf} - k_s)}. \end{array}\right\} \quad (9)$$

where μ_{nf} denotes the dynamic viscosity, ρ_{nf} is the density, k_{nf} represents the conductivity, α_{nf} the thermal diffusivity, and $\left(\rho C_p\right)_{nf}$ the heat capacitance.

The non-dimensional parameters are used as follows:

$r = \frac{\bar{R}}{d_o}, z = \frac{\bar{Z}}{L_o}, \beta = \frac{Q_o d_o^2}{k_f T_o}, w = \frac{\bar{W}}{w_o}, v = \frac{L_o \bar{R}}{\delta w_o}\bar{V}, d = \frac{\bar{d}}{L_o}, \bar{p} = \frac{w_o L_o \mu}{d_o^2} p,$

$Gr = \frac{g \propto d_o^2 \bar{T}_o \rho_{nf}}{w_o \mu_f}, \kappa = \frac{\mu_{nf}\, c}{\rho_{nf}\, g d_o^2}, \bar{\delta} = \frac{\delta}{d_o}, \Theta = \frac{\bar{T} - \bar{T}_o}{\bar{T}_o}.$ (10)

Obtaining Equations (11) - (14) with boundary conditions (14) - (16) with the aid of Equations (10) and (9) in Equations (2) to (8) and restrained stenosis $\left(\frac{\delta}{d_o} \ll 1\right) (\ll 1$) condition $\epsilon = \frac{d_o}{L_o} = o(1)$.

$\frac{\partial \mathrm{p}}{\partial r} = -\frac{\cos\theta}{\kappa}$ (11)

$\frac{dp}{dz} = \frac{1}{(1-\emptyset)^{2.5}} \frac{1}{r} \frac{\partial}{\partial r}\left(r \frac{\partial v}{\partial r}\right) + Gr\Theta + \frac{\sin\theta}{\kappa}$ (12)

$\frac{1}{r} \frac{\partial}{\partial r}\left(r \frac{\partial \Theta}{\partial r}\right) + \beta \left(\frac{k_{nf}}{k_f}\right) = 0$ (13)

With corresponding boundary conditions

$\frac{\partial u}{\partial r} = 0,\ \frac{\partial \Theta}{\partial r} = 0 \quad at \quad r = 0,$ (14)

$u = v_c,\ \Theta = 0 \ at \quad r = R(z),$ (15)

$\frac{\partial u}{\partial r} = \frac{\alpha}{\sqrt{D_a}}\left(v_s - v_p\right) \quad at \quad r = R(z),$ (16)

where $v_f = -\frac{D_a}{\mu}\frac{dp}{dz}$ represents the permeable boundary velocity, v_c signifies the slip velocity α denotes the slip parameter and D_a is the Darcy number, p symbolizes the pressure, β is the heat absorbing constraint , Gr the Grashof number, $\emptyset$ is volume fraction of nanoparticles, r is the radius, Θ the temperature, and v represents the velocity of the blood by Shailesh et al. (2011) and Dada and Babatunde (2021a).

III. Analysis

Resolving Equation (13) and it can be expressed as

$\frac{\partial}{\partial r}\left(r \frac{\partial \Theta}{\partial r}\right) = -\beta \left(\frac{k_{nf}}{k_f}\right) r$ (17)

Integrating Equation (17) with respect to r, in view of boundary condition (14) and (15) we have

$\Theta = -\beta \left(\frac{k_{nf}}{k_f}\right)(r^2 - R^2)$ (18)

Substituting Equation (18) into Equation (12), we have

$$\frac{\partial}{\partial r}\left(r \frac{\partial v}{\partial r}\right) = \frac{dp}{dz}(1-\emptyset)^{2.5} r + Gr\left(\beta \left(\frac{k_{nf}}{k_f}\right)(r^2 - R^2)\right) r - \frac{\sin\theta}{\kappa} r \quad (19)$$

Similarly, integrating Equation (19) with respect to r, in view of boundary conditions we have

$v = \left(-\frac{dp}{dz}\frac{L_1}{4} + \frac{Gr\Theta}{4} L_1 + \frac{\sin\theta}{4\kappa} L_1\right)(R^2 - r^2) + v_s$ (20)

where $L_1 = (1-\emptyset)^{2.5}$

Applying the boundary condition (16) on Equation (19), the slip velocity v_s can be determined as

$v_s = \left(\frac{dp}{dz} L_1 - Gr\Theta L_1 - \frac{\sin\theta}{\kappa} L_1\right)\frac{\sqrt{Da}}{2\alpha} R - \frac{Da}{\mu}\frac{dp}{dz}$ (21)

The expression of the volumetric flux is

$Q = 2\pi \int_0^{R(z)} vrdr,$ (22)

Substituting Equations (20) and (21) into Equation (22). Therefore, the solution of the volumetric flow flux is obtained as

$$Q = \frac{\pi}{8}\frac{dp}{dz}\left(L_1 R^4 + 4L_1 \frac{\sqrt{Da} R^3}{\alpha} - \frac{8Da R^2}{\mu}\right) + \frac{\pi Gr\Theta L_1}{8}\left(R^4 - \frac{4\sqrt{Da} R^3}{\alpha}\right) + \frac{\pi \sin\theta}{8\kappa}\left(R^4 - \frac{2\sqrt{Da} R^3}{\alpha}\right) \quad (23)$$

Therefore, from Equation (23), in term of $\frac{R(z)}{R_0}$, the pressure gradient of the blood of the arterial stenosis is obtained as

$$\frac{dp}{dz} = 8\frac{\left(Q - \frac{\pi Gr\,\Theta L_1}{8}\left(\mathrm{R}_0^4\left(\frac{R(z)}{R_0}\right)^4 - \frac{4\sqrt{Da}\,\mathrm{R}_0^3\left(\frac{R(z)}{R_0}\right)^3}{\alpha}\right) - \frac{\pi \sin\theta}{8\kappa}\left(\mathrm{R}_0^4\left(\frac{R(z)}{R_0}\right)^4 - \frac{2\sqrt{Da}\,\mathrm{R}_0^3\left(\frac{R(z)}{R_0}\right)^3}{\alpha}\right)\right)}{\pi\left(L_1 \mathrm{R}_0^4\left(\frac{R(z)}{R_0}\right)^4 + 4L_1\frac{\sqrt{Da}}{\alpha}\mathrm{R}_0^3\left(\frac{R(z)}{R_0}\right)^3 - \frac{8Da}{\mu}\mathrm{R}_0^2\left(\frac{R(z)}{R_0}\right)^2\right)} \quad (24)$$

The resolution of Equation (24) across the length of the artery is obtained as

$$\int_{p_1}^{p_2} dp = \frac{8}{\pi}\int_0^L \frac{\left(Q-\frac{\pi Gr\,\Theta L_1}{8}\left(\mathrm{R}_0^4\left(\frac{R(z)}{R_0}\right)^4-\frac{4\sqrt{Da}\,\mathrm{R}_0^3\left(\frac{R(z)}{R_0}\right)^3}{\alpha}\right)-\frac{\pi\sin\theta}{8\kappa}\left(\mathrm{R}_0^4\left(\frac{R(z)}{R_0}\right)^4-\frac{2\sqrt{Da}\,\mathrm{R}_0^3\left(\frac{R(z)}{R_0}\right)^3}{\alpha}\right)\right)}{\left(L_1\mathrm{R}_0^4\left(\frac{R(z)}{R_0}\right)^4+4L_1\frac{\sqrt{Da}}{\alpha}\mathrm{R}_0^3\left(\frac{R(z)}{R_0}\right)^3-\frac{8Da}{\mu}\mathrm{R}_0^2\left(\frac{R(z)}{R_0}\right)^2\right)}dz \qquad (25)$$

Then,

$$p_2-p_1 = \int_0^L \frac{\left(Q-\frac{\pi Gr\,\Theta L_1}{8}\left(\mathrm{R}_0^4\left(\frac{R(z)}{R_0}\right)^4-\frac{4\sqrt{Da}\,\mathrm{R}_0^3\left(\frac{R(z)}{R_0}\right)^3}{\alpha}\right)-\frac{\pi\sin\theta}{8\kappa}\left(\mathrm{R}_0^4\left(\frac{R(z)}{R_0}\right)^4-\frac{2\sqrt{Da}\,\mathrm{R}_0^3\left(\frac{R(z)}{R_0}\right)^3}{\alpha}\right)\right)}{\left(L_1\mathrm{R}_0^4\left(\frac{R(z)}{R_0}\right)^4+4L_1\frac{\sqrt{Da}}{\alpha}\mathrm{R}_0^3\left(\frac{R(z)}{R_0}\right)^3-\frac{8Da}{\mu}\mathrm{R}_0^2\left(\frac{R(z)}{R_0}\right)^2\right)}dz \qquad (26)$$

where p_1 and p_2 denote thee pressures at $z = 0$ and $z = L$.

The resistance to flow λ is defined by Babatunde and Dada (2021a) and Dhange et al. (2025) as

$$\lambda = \frac{p_2-p_1}{Q}$$

$$\lambda = \int_0^L \frac{T}{\left(L_1\mathrm{R}_0^4\left(\frac{R(z)}{R_0}\right)^4+4L_1\frac{\sqrt{Da}}{\alpha}\mathrm{R}_0^3\left(\frac{R(z)}{R_0}\right)^3-\frac{8Da}{\mu}\mathrm{R}_0^2\left(\frac{R(z)}{R_0}\right)^2\right)}dz \qquad (27)$$

and

$$\lambda = \int_0^d \frac{T}{\left(L_1\mathrm{R}_0^4\left(\frac{R(z)}{R_0}\right)^4+4L_1\frac{\sqrt{Da}}{\alpha}\mathrm{R}_0^3\left(\frac{R(z)}{R_0}\right)^3-\frac{8Da}{\mu}\mathrm{R}_0^2\left(\frac{R(z)}{R_0}\right)^2\right)}dz + \int_d^{d+\frac{3L_0}{2}} \frac{T}{\left(L_1\mathrm{R}_0^4\left(\frac{R(z)}{R_0}\right)^4+4L_1\frac{\sqrt{Da}}{\alpha}\mathrm{R}_0^3\left(\frac{R(z)}{R_0}\right)^3-\frac{8Da}{\mu}\mathrm{R}_0^2\left(\frac{R(z)}{R_0}\right)^2\right)}dz +$$

$$d+3L02LTL1\mathrm{R}04RzR04+4L1Daa\mathrm{R}03RzR03-8Da\mu\mathrm{R}02RzR02dz \qquad (28)$$

λ is the resistance to flow

where

$$T = 1-\frac{\pi Gr\,\Theta L_1}{8}\left(\mathrm{R}_0^4\left(\frac{R(z)}{R_0}\right)^4-\frac{4\sqrt{Da}\,\mathrm{R}_0^3\left(\frac{R(z)}{R_0}\right)^3}{\alpha}\right)-\frac{\pi\sin\theta}{8\kappa}\left(\mathrm{R}_0^4\left(\frac{R(z)}{R_0}\right)^4-\frac{2\sqrt{Da}\,\mathrm{R}_0^3\left(\frac{R(z)}{R_0}\right)^3}{\alpha}\right).$$

The stenosis exists in the region $d \le z \le d+\frac{3L_0}{2}$, where is no stenosis $\frac{\mathrm{R(z)}}{\mathrm{R}_0} = (\frac{mz}{R_0}+1)$from Equation (1). Therefore,

$\lambda =$

$$\int_0^d \frac{\Psi}{\left(L_1\mathrm{R}_0^4\left(\frac{mz}{R_0}+1\right)^4+4L_1\frac{\sqrt{Da}}{\alpha}\mathrm{R}_0^3\left(\frac{mz}{R_0}+1\right)^3-\frac{8Da}{\mu}\mathrm{R}_0^2\left(\frac{mz}{R_0}+1\right)^2\right)}dz +$$

$$dd+3L02TL1\mathrm{R}04RzR04+4L1Daa\mathrm{R}03RzR03-8Da\mu\mathrm{R}02RzR02dz+$$

$$d+3L02L\Psi L1\mathrm{R}04RzR04+4L1Daa\mathrm{R}03RzR03-8Da\mu\mathrm{R}02RzR02dz \qquad (29)$$

where

$$\Psi = 1-\frac{\pi Gr\,\Theta L_1}{8}\left(\mathrm{R}_0^4\left(\frac{mz}{R_0}+1\right)^4-\frac{4\sqrt{Da}\,\mathrm{R}_0^3\left(\frac{mz}{R_0}+1\right)^3}{\alpha}\right)-\frac{\pi\sin\theta}{8\kappa}\left(\mathrm{R}_0^4\left(\frac{mz}{R_0}+1\right)^4-\frac{2\sqrt{Da}\,\mathrm{R}_0^3\left(\frac{mz}{R_0}+1\right)^3}{\alpha}\right).$$

Resolving Equation (16) in the region of no stenosis, then the resistance to flow λ_N is obtained as

$$\lambda_N = \int_0^L \frac{\Psi}{\left(L_1\mathrm{R}_0^4\left(\frac{mz}{R_0}+1\right)^4+4L_1\frac{\sqrt{Da}}{\alpha}\mathrm{R}_0^3\left(\frac{mz}{R_0}+1\right)^3-\frac{8Da}{\mu}\mathrm{R}_0^2\left(\frac{mz}{R_0}+1\right)^2\right)}dz \qquad (30)$$

In dimensionless form, the resistance to flow can be expressed as

$$\bar{\lambda} = \frac{\lambda}{\lambda_N} \tag{31}$$

Expression of the wall shear stress can be obtained as

$$\tau_R = -\left(\frac{R}{2}\right)\frac{\partial p}{\partial z} = -\left\{4\frac{\left(Q-\frac{\pi Gr\,\Theta L_1}{8}\left(\mathrm{R}_0^4\left(\frac{R(z)}{R_0}\right)^4-\frac{4\sqrt{Da}\,\mathrm{R}_0^3\left(\frac{R(z)}{R_0}\right)^3}{\alpha}\right)-\frac{\pi\sin\theta}{8\kappa}\left(\mathrm{R}_0^4\left(\frac{R(z)}{R_0}\right)^4-\frac{2\sqrt{Da}\,\mathrm{R}_0^3\left(\frac{R(z)}{R_0}\right)^3}{\alpha}\right)\right)}{\pi\left(L_1\mathrm{R}_0^3\left(\frac{R(z)}{R_0}\right)^3+4L_1\frac{\sqrt{Da}}{\alpha}\mathrm{R}_0^2\left(\frac{R(z)}{R_0}\right)^2-\frac{8Da}{\mu}R_0\left(\frac{R(z)}{R_0}\right)\right)}\right\} \tag{32}$$

If $\frac{R(z)}{R_0} = (\frac{mz}{R_0} + 1)$, Equation (31) can be obtained as

$$\tau_N = -\left\{4\frac{\left(Q-\frac{\pi Gr\,\Theta L_1}{8}\left(\mathrm{R}_0^4\left(\frac{mz}{R_0}+1\right)^4-\frac{4\sqrt{Da}\,\mathrm{R}_0^3\left(\frac{mz}{R_0}+1\right)^3}{\alpha}\right)-\frac{\pi\sin\theta}{8\kappa}\left(\mathrm{R}_0^4\left(\frac{mz}{R_0}+1\right)^4-\frac{2\sqrt{Da}\,\mathrm{R}_0^3\left(\frac{mz}{R_0}+1\right)^3}{\alpha}\right)\right)}{\pi\left(L_1\mathrm{R}_0^3\left(\frac{mz}{R_0}+1\right)^3+4L_1\frac{\sqrt{Da}}{\alpha}\mathrm{R}_0^2\left(\frac{mz}{R_0}+1\right)^2-\frac{8Da}{\mu}R_0\left(\frac{mz}{R_0}+1\right)\right)}\right\} \tag{33}$$

In dimensionless form, the wall shear stress can be expressed

$$\bar{\tau} = \frac{\tau_R}{\tau_N} \tag{34}$$

IV. The streamline function

The streamline flow in fluid dynamic is the movement of particles of the fluid that follows a specified order moving in a straight line parallel to the tube wall in a way that the adjacent layers slide past each other likes playing cards. The stream function (ω) of the blood flow can be obtain mathematically as integral of $v = \frac{1}{r}\frac{\partial \omega}{\partial r}$ with $\omega = 0$ at $r = R(z)$, then the stream function is given by:

$$\omega = \int_0^{R(z)} rvdr \tag{35}$$

Substituting Equations (20) and (21) into Equation (35) and integrate, we have:

$$\omega = \left(-\frac{dp}{dz}\frac{L_1}{4} + \frac{Gr\Theta}{4}L_1 + \frac{\sin\theta}{4\kappa}L_1\right)\left(\frac{R^4}{2} - \frac{R^4}{4}\right) + \left(\frac{dp}{dz}L_1 - Gr\Theta L_1 - \frac{\sin\theta}{\kappa}L_1\right)\frac{\sqrt{Da}}{2\alpha}\frac{R^3}{2} - \frac{Da}{\mu}\frac{dp}{dz}\frac{R^2}{2} \tag{36}$$

Table 1: Thermo-physical properties of base fluid and nanoparticle

Property	Basa fluid (Blood)	Alumina (Al_2O_3)	Ferric Oxide (Fe_2O_3)
ρ (kg/m^3)	1063	3970	4000
K(W/mK)	0.492	40	2
$C_p(J/kgK)$	3594	765	700
$\xi(K^{-1})$	18000	85000	-

V. Discussion of numerical results

A series of computations has been carried out on the effects of the pertaining blood flow parameters. We took the value of the parameter from Babatunde and Dada (2021a), Haris et al., (2024) and Dhange et al., (2025).

And are considered as $L = 5, l = 1, L = 2.0, Q = 0.1, d = 0.5, R_0 = 0.5, \frac{\delta}{R_0} = 0.1 - 0.5, \beta = 5, 10 \; and \; 15, Gr = 2, \kappa = 0.8, \theta = \frac{\pi}{6}, \phi = 0.01, \varphi = 0.03, \alpha = 0.1, \sqrt{(D_a)} = 0.1, \mu = 0.3.$

Figures 2-7 Display the relationship between the velocity and radial direction for different values of heat absorption constant (β), Darcy number (Da), Grashof number (Gr), slip parameter (α), tapered angle (φ) and volume fraction of nanoparticles (ϕ). However, the velocity increases as heat absorption, Darcy number, Grashof number, tapering angle moves up, but reverse is the case for both slip parameter and volume fraction of the nanoparticles. More so, ferric oxide (Fe_2O_3) reacted to the flow than Alumina (Al_2O_3).

Figures 8-9 Display the relationship between temperature and radial direction for different values of heat absorption constant (β) and the tapering (ϕ). However, the temperature accelerates at both cases and ferric oxide (Fe_2O_3) reacted to the flow than Alumina (Al_2O_3).

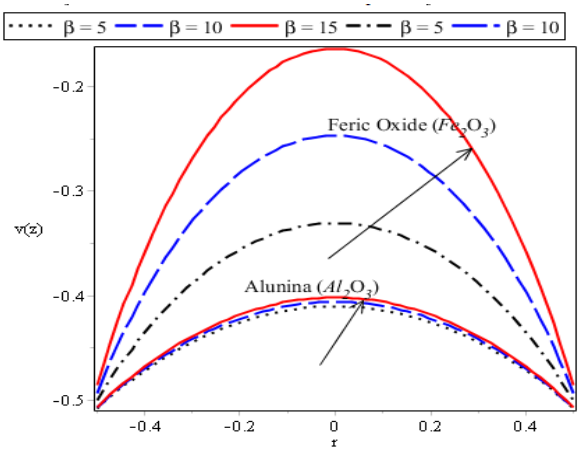

Figure 2: Illustrate velocity against radial direction

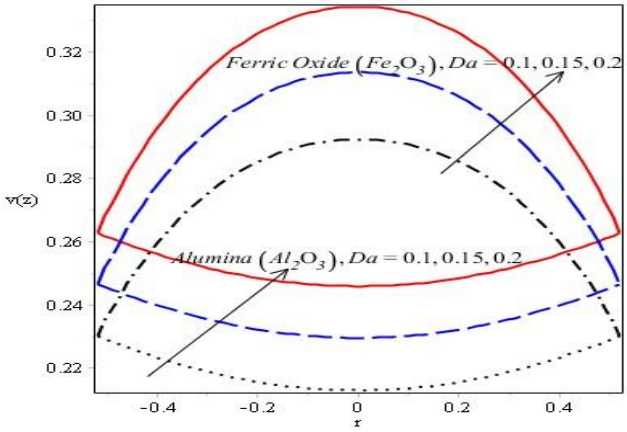

Figure 3: Illustrate velocity against radial direction

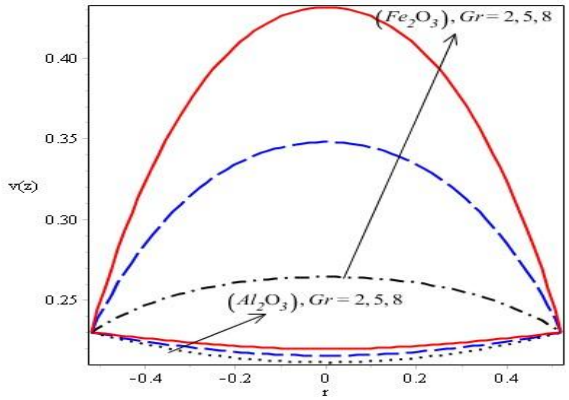

Figure 4: Illustrate velocity against radial direction

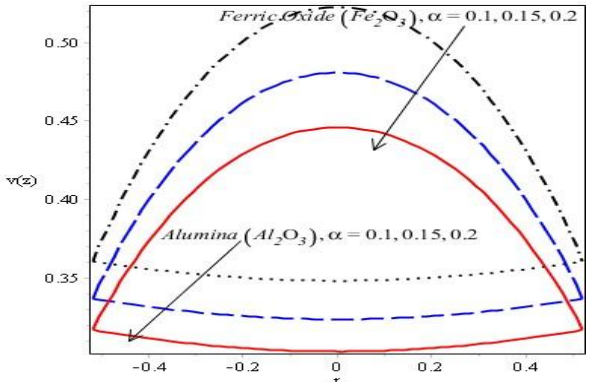

Figure 5: Illustrate velocity against radial direction

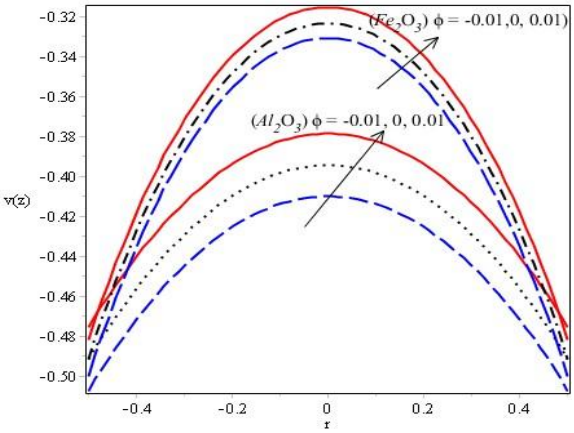

Figure 6: Illustrate velocity against radial direction

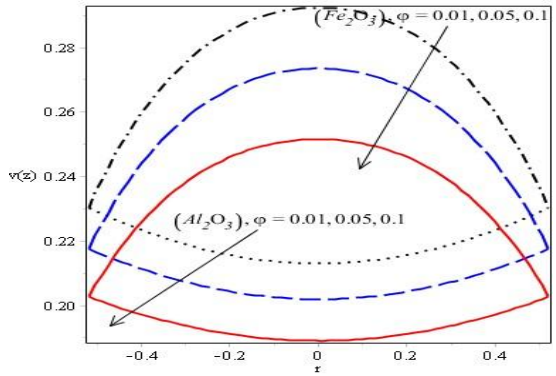

Figure 7: Illustrate velocity against radial direction

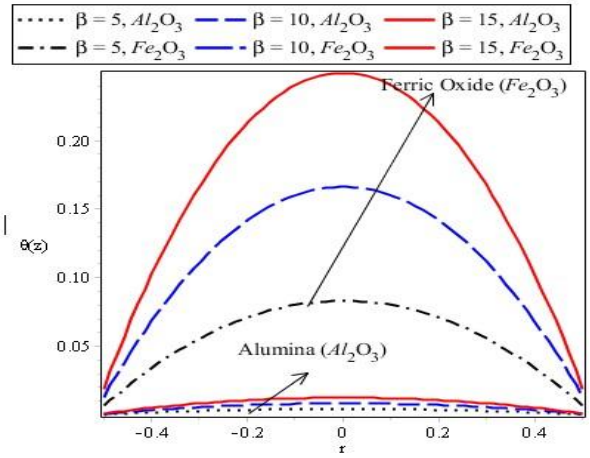

Figure 8: Illustrate temperature against radial direction

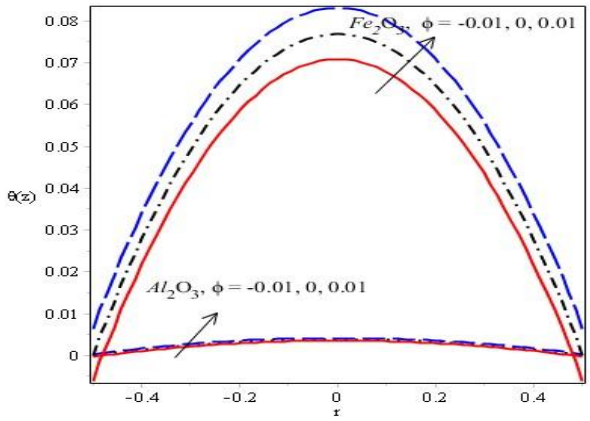

Figure 9: Illustrate temperature against radial direction

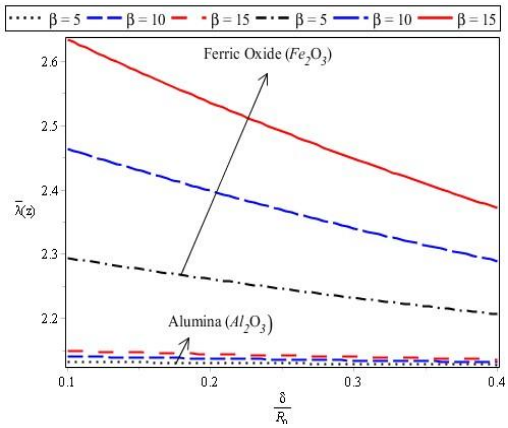

Figure 10: Illustrate resistance to flow against stenosis height

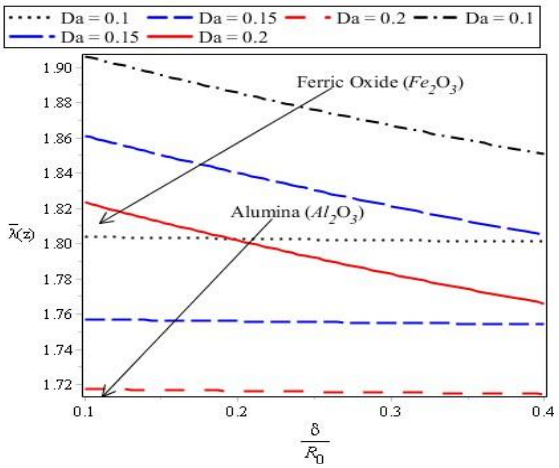

Figure 11: Illustrate resistance to flow against stenosis height

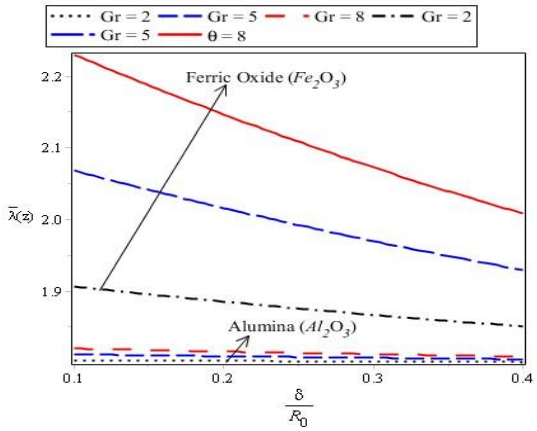

Figure 12: Illustrate resistance to flow against stenosis height

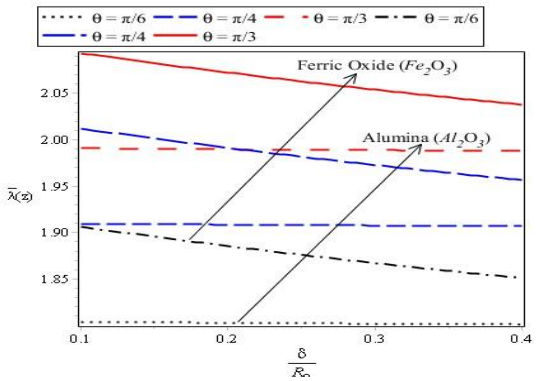

Figure 13: Illustrate resistance to flow against stenosis height

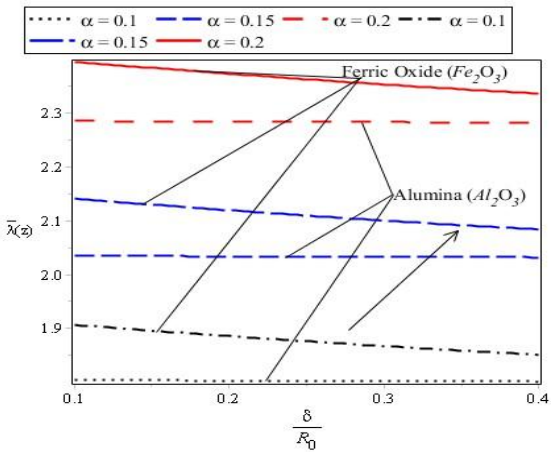

Figure 14: Illustrate resistance to flow against stenosis height

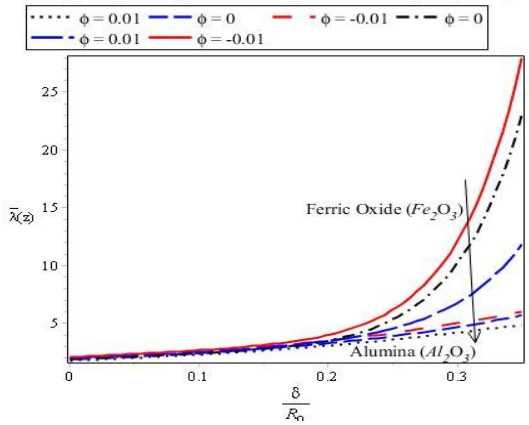

Figure 15: Illustrate resistance to flow against stenosis height

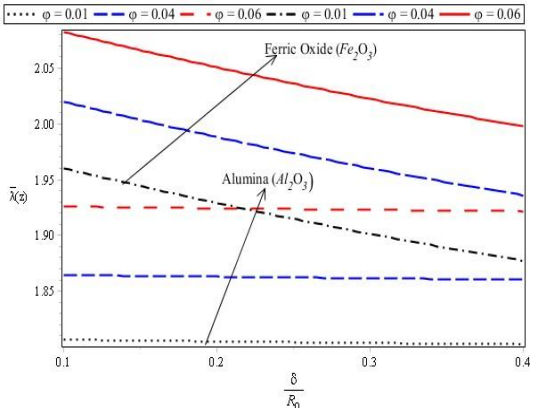

Figure 16: Illustrate resistance to flow against stenosis height

Figures 10-16 Display the dynamics of the resistance to flow with stenosis height for different values of heat absorption constant (β), Darcy number (Da), Grashof number (Gr), inclination angle (θ), slip parameter (α), tapered angle (φ) and volume fraction of nanoparticles (ϕ). However, the resistance to flow increases as heat absorption, Grashof number, inclined angle, slip parameter and tapering angle moves up, but reverse is the case for both Darcy number and volume fraction of the nanoparticles.

Figures 17-24 Display the relationship between the wall shear stress and z-direction for various values of heat absorption constant (β), Darcy number (Da), tapered angle (φ), Grashof number (Gr), inclination angle (θ), slip parameter (α), stenosis height (δ) and volume fraction of nanoparticles (ϕ). However, the wall shear stress decreases at all the cases except in figure (23) that it rises with ferric oxide (Fe_2O_3). More so, in this case Alumina (Al_2O_3) reacted to the flow than Ferric oxide (Fe_2O_3). Figures 25 and 26 show the streamline of the flows.

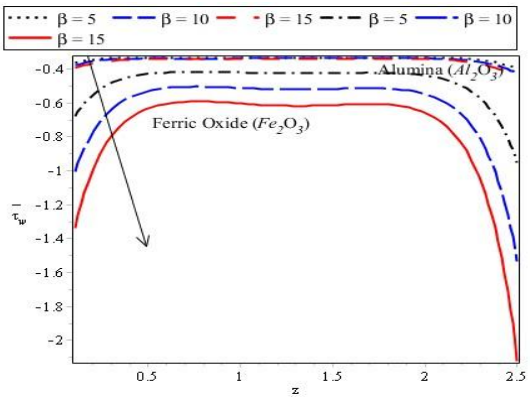

Figure 17: Illustrate wall shear stress against z-direction

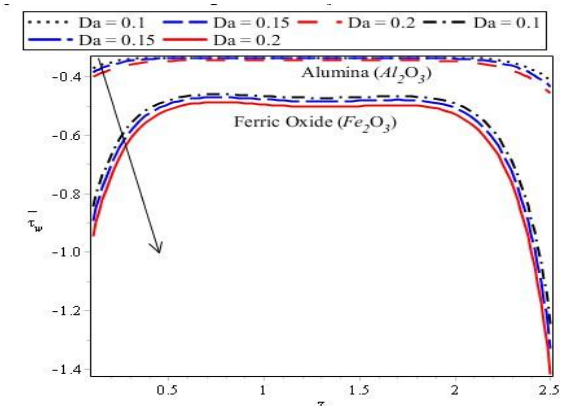

Figure 18: Illustrate wall shear stress against z-direction

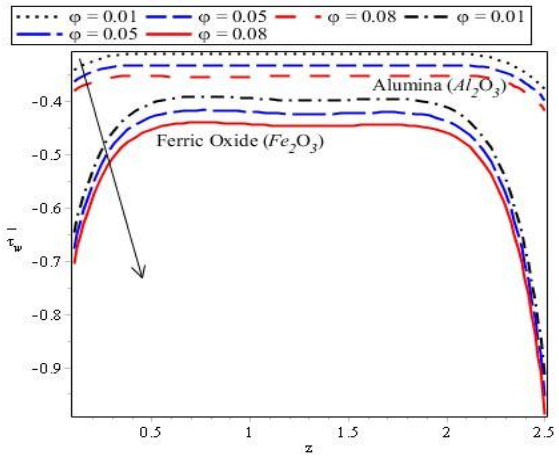

Figure 19: Illustrate wall shear stress against z-direction

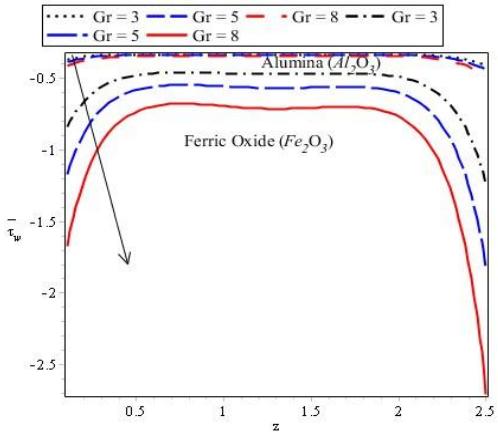

Figure 20: Illustrate wall shear stress against z-direction

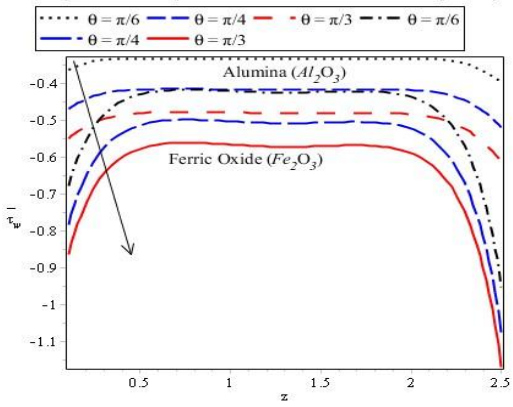

Figure 21: Illustrate wall shear stress against z-direction

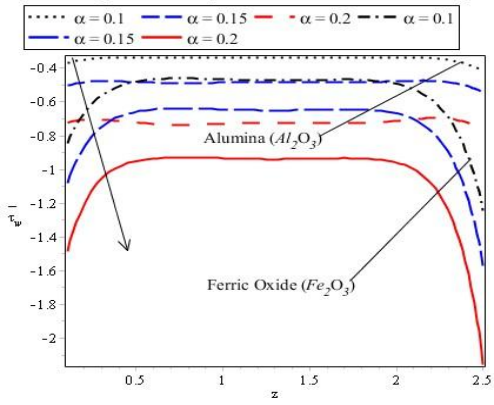

Figure 22: Illustrate wall shear stress against z-direction

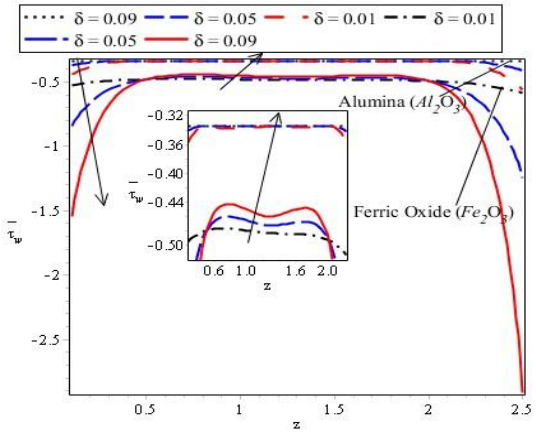

Figure 23: Illustrate wall shear stress against z-direction

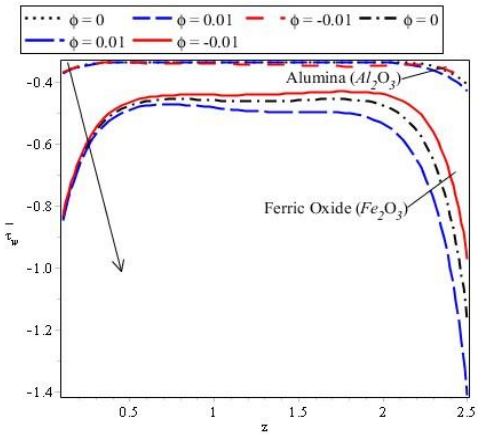

Figure 24: Illustrate wall shear stress against z-direction

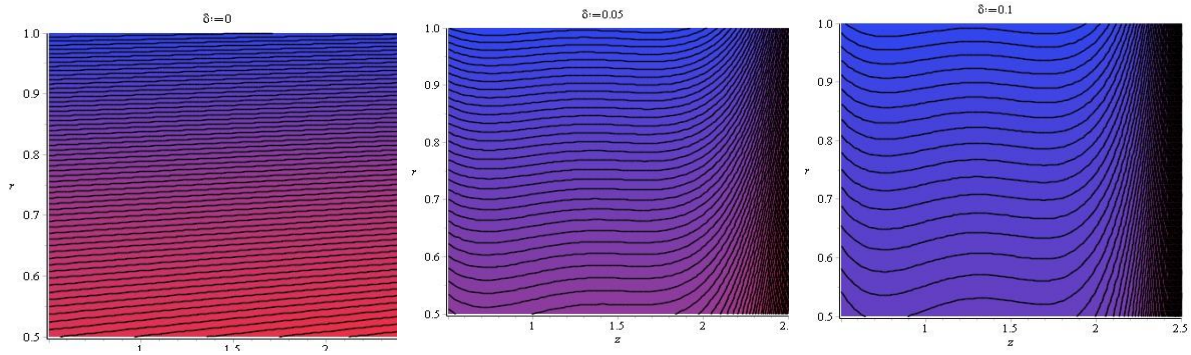

Figure 25: Illustrate streamline of the flow for stenosis height $\delta = 0, 0.05$ *and* 0.1 at $\varphi = 0.02$.

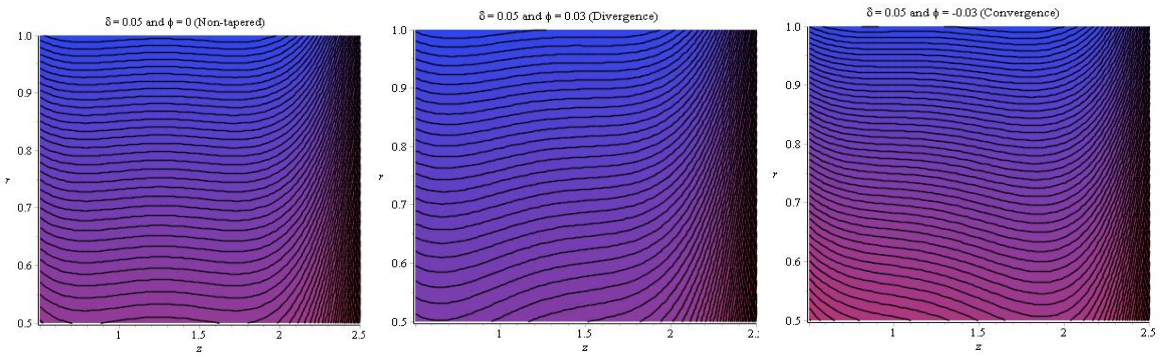

Figure 26: Illustrate streamline of the flow for tapered angle $\varphi = 0, 0.03$ and -0.03 at $\delta = 0.05$.

VI. CONCLUSION

The hemodynamic behavior of blood flow in a tapered and overlapping stenotic vessel through a permeable wall with nanoparticles in an inclined plain has been discussed in this study. The results are itemized below:

1. It was found that velocity profile enhances with an hike in Darcy number, Grashof number and heat absorption, but it drops with increasing in the values of slip parameter and volume fraction of nanoparticles
2. The temperature profile moves in favor of both heat absorption and tapered angle
3. It was observed that resistance to flow speedup with increasing in heat absorption, Grashof number, and slip parameter
4. The wall shear stress decelerates as Darcy number, slip parameter, heat absorption, and volume fraction of nanoparticles rise.
5. Alumina (Al_2O_3) reacted to the flow than ferric oxide (Fe_2O_3) in wall shear stress but converse is the case for both velocity and temperature profiles.

REFERENCES

[1]. A. Ahmed, A. and Nadeem, S. 2016. The study of (Cu, $TiO2$, $Al2O3$) nanoparticles as anti-microbials of blood flow through diseased arteries. J Mol Liq. 216: 615–23. doi:10.1016/j.molliq.2016.01.059.

[2]. Sarwar, L., Hussain, A., Fernandez-Gamiz U, Akbar S, Rehman A, Sherif ESM., Thermal enhancement and numerical solution of blood nanofluid flow through stenotic artery. Sci Rep. 2022; 12(1):17419. doi:10.1038/s41598-022-20267-8.

[3]. Ellahi, R., Rahman, S. U. and Mudassar, M. 2024. Mathematical model of non-Newtonian fluid micro-polar fluid in arterial blood flow through composite stenosis. Applied Mathematical and Information Sciences. 2014. Vol. 8(4): 1567 - 1573.

[4]. Mofrad, M.R.K., Wada S., Myers, J.G., and Ethier, C.R., 2005. Mass transport and fluid flow in stenosis arteries: Axisymmetric and asymmetric models. Inter. Journal of Health and mass transfer. 48, 907 - 918.

[5]. Srivastav, R. K., 2014. Mathematical Model of Blood Flow through a Composite Stenosis in Catheterized Artery with Permeable Wall, Application and applied: Intern. J., 2014. Vol. 9, Issue 1.

[6]. Babatunde, A. J. and Dada, M. S. 2021a. Effects of Hematocrit level on blood flow through a tapered and overlapping stenosed artery with porosity. Journal of heat and mass transfer Research 2021. 8:39-47.

[7]. Babatunde, A. J., Oyekunle, T. L. , Danas J. Y., and Mohammed M. T., 2021b. Effects of Hematocrit and Heat transfer in Magnetohydrodynamic blood flow through a vertically tapered and overlapping stenosed artery. JOSIT.

[8]. Babatunde, A.J. and Dada, M. S. 2023. Magnetic effects on unsteady Non-Newtonian blood flow through a tapered and overlapping stenosed artery. Appl and Applied Mathematics: An International Journal (AAM). Vol. 19, Issue 1

[9]. Jamil, D.F, Roslan, R., Abdulhameed, M., Che-Him N., Sufahani S., Mohamad M., 2018. Unsteady blood flow with nanoparticles through stenosed arteries in the presence of periodic body acceleration. J Phys: Conf Ser. 995:012032. doi:10.1088/1742-6596/995/1/012032.

[10]. Vasu, B., Dubey, A., Beg OA, Gorla, RSR. 2020. Micropolar pulsatile blood flow conveying nanoparticles in stenotic tapered artery: non-Newtonian pharmacodynamics simulation. ComputBiol Med. 126:104025, dio:10.1016/j.compbiomed.2020.104025.

[11]. Shazad, F., Jamshed, W., Aslam, F., Bashir, R., Tag, El Din ESM, Khalifa, HAEW. 2022. MHD pulsaltile flow of blood-based silver and gold nanoparticles between two concentric cylinders, Symmetry. 14(11):2253, dio:10.3390/sym14112254.

[12]. Karmakar, D., Lahiri, P., MinakshiBedi, Aritri G., Alok Ghosh, AnanyaBarui, S. Kumar Varshney, Basudev L., and S. Sengupta. 2023. FTIR microspectroscopy and multivariate analysis facilitate identification of dynamic changes in epithelial to mesenchymal transition induced by TGF-b in prostate cancer cell. Journal of Cellular Biochemistry, Vol. 124, issue 6. Pp. 849-860.

[13]. Muthtamilselvan, M., Gifteena Hingis, Y., 2023. Flow characteristics of gold nanoparticles and microorganisms in a multistenotic artery treated with a catheter. Aust J Mech Eng. 1–16. doi:10.1080/14484846.2023.2290335.

[14]. Sharma, B. K., Khanduri, U., Mishra, N.K., Albaijan, I., Perez, L.M. 2023. Entropy generation optimization for the electroosmotic MHD fluid flow over the curved stenosis artery in the presence of thrombosis. Sci Rep. 13(1):15441. doi:10.1038/s41598-023-42540-0.

[15]. HarisAlamZuberi, Madan Lal, Amol Singh, Nurul Amira Zainal and Ali J. Chamkha, 2024. Numerical simulation of blood flow dynamics in a stenosed artery enhanced by copper and alumina nanoparticles. Comp. Modeling in Eng. And Sci. DOI: 10.32604/cmes.2024.056661.

[16]. Mekheimer, Kh.S. and El Kot M.A., 2012. Mathematical modelling of unsteady flow of a Sisko fluid through an anisotropically tapered elastic arteries with time-variant overlapping stenosis. Applied Mathematical Modelling: 36, 5393-5407.

[17]. Shailesh Mishra, S. U., Siddiqui, and Amit Medhavi. 2011. Blood flow through a composite stenosis in an artery with permeable wall. Appli and Applied Mathe: an International Journal (AAM). Vol. 6, Iss. 1, Article 5.

[18]. Dhange, M., Salgare, S., Kusal K. Das, Ebenezer Bonyah, HabtuAlemayehu. 2015. Hemodynamic properties of blood flow in an angled overlying stenosed blood vessel via force field and gold nanoparticle suspension. Scientific African 28, e02652. doi.org/10.1016/j.sciaf.2025.e02652